

Two-dimensional model for the double glass naturally ventilated window

K.A.R. Ismail ^{a,*}, J.R. Henriques ^b

^a *Depto. de Engenharia Térmica e de Fluidos—FEM-UNICAMP CP: 6122, CEP 13083-970 Campinas, SP, Brazil*

^b *Depto. de Engenharia Mecânica—DEMEC, UFPE-Avenida Acadêmico Hélio Ramos, S/N. CEP 50740-530, Recife, PE, Brazil*

Received 19 August 2003; received in revised form 13 September 2004

Available online 11 November 2004

Abstract

This paper presents a mathematical model and the results of numerical simulations of a double sheet ventilated glass window. The incident solar radiation heats up the air between the glass sheets creating buoyancy forces that induces upward flow of air. The two-dimensional transient model is formulated based upon the fundamental equations of mass conservation, momentum and energy, the associated constant and time varying boundary conditions and is solved by finite difference approach and the ADI (alternating direction implicit) scheme. The numerical grid and the time increment were optimized and the numerical results were validated against available data. Results of the temperature field along and across the channel are obtained for different spacing between the glass sheets and incident radiation conditions. The effects on the solar heat gain coefficient and the shading coefficient were also presented and discussed.

© 2004 Elsevier Ltd. All rights reserved.

Keywords: Ventilated glass window; Double glass window; Numerical simulation; Natural convection

1. Introduction

Windows are usually the weak barriers which separate the external and internal ambient. In cold climates they are usually responsible for 10–25% of the heat lost from heated ambient. In hot climates, the excess of solar radiation penetrating through the glass windows usually lead to excessive cooling load. For these and other reasons a great deal of research work and engineering developments were devoted to creating efficient and

thermally effective windows capable of maintaining adequate level of thermal comfort.

Windows having selective solar radiation characteristics are examples of thermally efficient windows. The selective properties due to deposited film on glass sheets allow changing the transmittance reflectance and absorptance of the window.

These films can be designed to absorb or reflect according to the wavelength of the incident radiation. A vast review of technologies of selective films is reported by Lampert [1]. Low emissivity glass windows are also of low absorption coefficient and high reflectivity in the infrared range as in Daklen [2], Sebastian and Sivaramakrishnan [3] and Sebastian and Pattabi [4]. Mathematical models to investigate the thermal behavior of windows fitted with films for solar radiation

* Corresponding author. Tel.: +55 19 37883214; fax: +55 19 7883722.

E-mail addresses: kamal@fem.unicamp.br (K.A.R. Ismail), rjorgeh@demec.ufpe.br (J.R. Henriques).

Nomenclature

A	area [m ²]
c	specific heat [kJ/kg K]
e	glass thickness [m]
F	solar heat gain coefficient
g	acceleration of gravity [m/s ²]
Gr	Grashof number
h	heat transfer coefficient [W/m ² K]
I_o	solar radiation [W/m ²]
k	thermal conductivity [W/m K]
m_v	number of intervals in the glass along the y -direction
m	number of intervals along the y -direction
n_1	number of intervals in the adiabatic region (entry or exit) along the x -direction
n	number of intervals in the glass along the x -direction
p	pressure [N/m ²]
q	heat flux [W/m ²]
Re	Reynolds number
SC	shading coefficient
T	temperature [°C]
t	time [s]
u	velocity in the x direction [m/s ¹]
\bar{u}	average velocity at entry of the channel [m/s ¹]
U	overall heat transfer coefficient [W/m ² K ¹]
v	velocity in the y direction [m/s ¹]
x, y	cartesian coordinates

Greek symbols

μ	viscosity [kg/m s]
α	thermal diffusivity [m ² /s ¹]
α_1, α_2	absortance coefficient in the external and internal glass
β	coefficient of volumetric thermal expansion [1/K]
ρ	density [kg/m ³]
τ	transmittance coefficient
ε	emissivity
σ	Stefan–Boltzmann constant, 5.57×10^{-8} [W/m ² K ⁴]
Δ	increment

Subscripts

c	channel or cavity
conv	convection
ext	external
f	fluid
fr	frame
i	grid position in the x direction
int	internal
j	grid position in the y direction
max	maximum
min	minimum
rad	radiation
v	glass
w	wall
∞	ambient

control were proposed by Alvarez et al. [5,6] for the steady state and transient conditions.

High performance is also achieved by using evacuated glass panels where heat transfer by conduction and convection is greatly reduced as in Sullivan et al. [7], Lenzen and Collins [8] and the excellent review on evacuated windows by Collins and Simko [9].

The use of absorbing gases filling the gap between glass sheets appears to be an alternative solution for thermally insulated glass windows as in Reilly et al. [10], Bernier and Bourret [11] and Zhao et al. [12]. Other glass window system use alternative filling materials instead of absorbing gases such as silica aerogel by Einarsrud et al. [13] and Duer and Svendsen [14], phase change materials as in Castro [15], Henríquez [16], Ismail and Henríquez [17,18] and Manz et al. [19]. Rottkay et al. [20] and Seeboth et al. [21] investigated the use of chromogenic materials in windows. The basic characteristic of such materials is its ability to change its optical properties if stimulated by light (photochromics), heat (thermochromics) or by electric currents

(electrochromics). These materials are still in the laboratory tests.

Fluid flow in the gap between the glass sheets of a double panel window offers an option for thermally efficient windows. Experimental work on ventilated windows was reported by Onur et al. [22] and TEPCO (Tokyo Electric Power Company) [23].

Etzion and Erell [24] presented a new concept of ventilated window while Tanimoto and Kimura [25] presented a calculation procedure for ventilated windows with a curtain and venetian. Haddad and Elmahdy [26] developed a model and a computational program to simulate the performance of a conventional window and a ventilated window. Zhang et al. [27] reported a study of the effect of venetian installed into a cavity formed by two glass sheets. None complex models involving transient phenomena and two dimensional heat processes were presented by Belharat et al. [28], Abreu et al. [29], Larsson et al. [30] and Henríquez [31].

In this paper the thermal behavior of a ventilated glass window is numerically investigated and the

mechanisms of heat transfer through the glass window are simulated. The window is composed of two parallel sheets of glass forming a channel through which air flows. The incident solar radiation and the temperature difference between the external and internal ambient are responsible for the upward airflow. The proposed model is two dimensional and transient with the heat flow mechanism on the external side assumed to be by convection and long wave radiation and on the internal side by convection and radiation. The incident solar radiation and the internal ambient temperature are considered to vary with time following a model that takes into account the geographical and meteorological conditions.

The treatment of natural convection in the channel requires the simultaneous solution of the equations of conservation of energy, momentum and mass. These equations are subject to a set of assumptions and simplifications. As a result of the numerical simulations it was possible to obtain details of the flow field in the channel, temperature distributions in the fluid flow field and the glass sheets. By adequate treatment of the results, the solar heat gain coefficient and the shading coefficient were determined.

2. Formulation of the problem

Basically the problem to be treated here is of flow induced by natural convection in a channel formed by two parallel walls with non-symmetric heating as shown in Fig. 1. The heating is due to incident solar radiation and convection and also radiation exchange between the walls and the internal and external ambient. Air is induced up into the channel by the buoyancy forces

due to the thermal effects. The adiabatic regions at entry and exit are included so as to enable to specify the boundary conditions. The problem is a two-dimensional transient laminar incompressible flow except for the buoyancy effects where the Boussinesq approximation is applied.

The mass conservation equation can be written as

$$\frac{\partial u}{\partial x} + \frac{\partial v}{\partial y} = 0 \tag{1}$$

The equation of motion in the x and y directions can be written as

$$\frac{\partial u}{\partial t} + \frac{\partial(uu)}{\partial x} + \frac{\partial(vu)}{\partial y} = -\frac{1}{\rho} \frac{\partial p}{\partial x} + \frac{\mu}{\rho} \frac{\partial^2 u}{\partial x^2} + \frac{\mu}{\rho} \frac{\partial^2 u}{\partial y^2} - g \tag{2}$$

$$\frac{\partial v}{\partial t} + \frac{\partial(uv)}{\partial x} + \frac{\partial(vv)}{\partial y} = -\frac{1}{\rho} \frac{\partial p}{\partial y} + \frac{\mu}{\rho} \frac{\partial^2 v}{\partial x^2} + \frac{\mu}{\rho} \frac{\partial^2 v}{\partial y^2} \tag{3}$$

The pressure term in Eqs. (2) and (3) can be expressed in terms of two parts, one due to hydrostatic pressure at a x position in the channel ($-\rho_\infty g x$) and the other part is due to the fluid motion p_m and hence one can write

$$p = p_m - \rho_\infty g x \tag{4}$$

Differentiating Eq. (4) in the x and y directions one can write

$$\frac{\partial p}{\partial x} = \frac{\partial p_m}{\partial x} - \rho_\infty g \tag{5}$$

$$\frac{\partial p}{\partial y} = \frac{\partial p_m}{\partial y} \tag{6}$$

Substituting Eqs. (5) and (6) into Eqs. (2) and (3) leads to

$$\frac{\partial u}{\partial t} + \frac{\partial(uu)}{\partial x} + \frac{\partial(vu)}{\partial y} = -\frac{1}{\rho} \frac{\partial p_m}{\partial x} + \frac{\mu}{\rho} \frac{\partial^2 u}{\partial x^2} + \frac{\mu}{\rho} \frac{\partial^2 u}{\partial y^2} - g \left(\frac{\rho - \rho_\infty}{\rho} \right) \tag{7}$$

$$\frac{\partial v}{\partial t} + \frac{\partial(uv)}{\partial x} + \frac{\partial(vv)}{\partial y} = -\frac{1}{\rho} \frac{\partial p_m}{\partial y} + \frac{\mu}{\rho} \frac{\partial^2 v}{\partial x^2} + \frac{\mu}{\rho} \frac{\partial^2 v}{\partial y^2} \tag{8}$$

The Boussinesq approximation can be written in the form

$$\rho - \rho_\infty \cong -\rho\beta(T - T_\infty) + \dots \tag{9}$$

Which when substituted into Eq. (7) one can obtain

$$\frac{\partial u}{\partial t} + \frac{\partial(uu)}{\partial x} + \frac{\partial(vu)}{\partial y} = -\frac{1}{\rho} \frac{\partial p_m}{\partial x} + \frac{\mu}{\rho} \frac{\partial^2 u}{\partial x^2} + \frac{\mu}{\rho} \frac{\partial^2 u}{\partial y^2} + g\beta(T - T_\infty) \tag{10}$$

The two dimensional transient energy equation without the viscous dissipation term can be written as

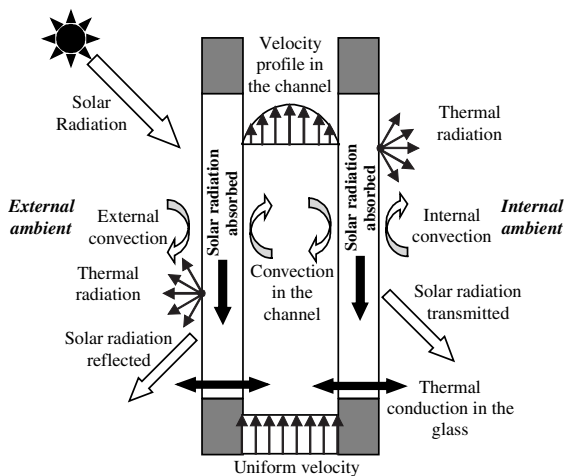


Fig. 1. Layout of natural convection a ventilated window.

$$\frac{\partial T}{\partial t} + \frac{\partial}{\partial x}(uT) + \frac{\partial}{\partial y}(vT) = \alpha \left(\frac{\partial^2 T}{\partial x^2} + \frac{\partial^2 T}{\partial y^2} \right) - \frac{1}{\rho c} \frac{\partial I}{\partial y} \quad (11)$$

The term $(-\partial I/\partial y)$ in Eq. (11) will be used to compute the solar radiation absorbed by the glass sheets forming the channel and can be expressed in terms of the radiation attenuation along the rays' path across the glass sheets. When applying the energy equation to the flow region, the source term $(-\partial I/\partial y)$ will be zero since it is assumed that the airflow is a non-participating medium and consequently is transparent to solar radiation.

Fig. 2 shows the general layout of the problem and the associated boundary conditions

- Internal surfaces of the channel

The non-slip condition is

$$u = v = 0 \text{ in } y = y_1 \text{ and } 0 \leq x \leq x_3 \quad (12)$$

$$u = v = 0 \text{ in } y = y_2 \text{ and } 0 \leq x \leq x_3 \quad (13)$$

- Channel entry

Assume uniform velocity along x and velocity zero along y

$$u = \bar{u}, v = 0 \text{ in } x = 0 \text{ and } y_1 \leq y \leq y_2 \quad (14)$$

The boundary condition for the pressure obtained by applying Bernoulli's equation, $p - p_{atm} = -0.5\rho\bar{u}^2$ where \bar{u} is the average velocity. Alternatively one can consider that the pressure at entry is equal to the atmospheric pressure as done by Marcondes and Maliska [32].

$$p = p_{atm}, \text{ in } x = 0 \text{ and } y_1 \leq y \leq y_2 \quad (15)$$

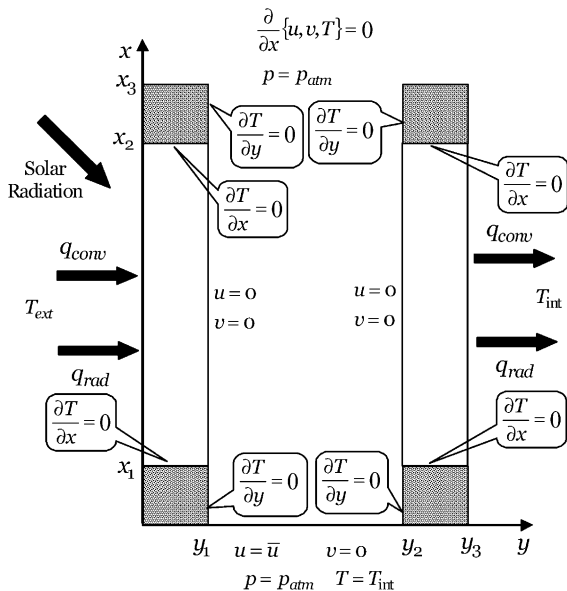


Fig. 2. Layout of the problem and the associated boundary conditions.

- Channel exit

At exit assume that the flow is fully developed and that the pressure is atmospheric

$$\frac{\partial u}{\partial x} = 0; \frac{\partial v}{\partial x} = 0 \text{ and } p = p_{atm} \text{ in } x = x_3, y_1 \leq y \leq y_2 \quad (16)$$

The boundary conditions for the energy equations are:

- Surface in contact with the external ambient

The boundary condition on the external surface is due to radiation and convection heat transfer between the glass surface and the external air. Hence the energy balance can be written as

$$q_{y=0} = -k_v \frac{\partial T}{\partial y} \Big|_{y=0} = h_{ext}(T_{ext} - T_{y=0}) + \sigma \epsilon (T_{ext}^4 - T_{y=0}^4) \quad (17)$$

valid for $y = 0$ and $x_1 \leq x \leq x_2$.

- Surfaces in contact with the internal ambient

In a similar manner one can write

$$q_{y=y_3} = -k_v \frac{\partial T}{\partial y} \Big|_{y=y_3} = h_{int}(T_{y=y_3} - T_{int}) + \sigma \epsilon (T_{y=y_3}^4 - T_{int}^4) \quad (18)$$

valid for $y = y_3$ and $x_1 \leq x \leq x_2$.

- Adiabatic region inside the channel

At the adiabatic entry and exit regions one can write

$$\frac{\partial T}{\partial y} = 0 \text{ for } y = y_1, 0 \leq x \leq x_1 \text{ and } x_2 \leq x \leq x_3 \quad (19)$$

$$\frac{\partial T}{\partial y} = 0 \text{ for } y = y_2, 0 \leq x \leq x_1 \text{ and } x_2 \leq x \leq x_3 \quad (20)$$

- Adiabatic region within the glass sheets.

The boundary conditions at the bottom and top extremities of the glass sheet can be written as

$$\frac{\partial T}{\partial x} = 0 \text{ for } x = x_1, 0 \leq y \leq y_1, y_2 \leq y \leq y_3 \quad (21)$$

$$\frac{\partial T}{\partial x} = 0 \text{ for } x = x_2, 0 \leq y \leq y_1, y_2 \leq y \leq y_3 \quad (22)$$

- The channel entry and exit

The air temperature at entry is assumed to be equal to the internal ambient temperature

$$T = T_{int} \text{ for } x = 0 \text{ and } y_1 \leq y \leq y_2 \quad (23)$$

While at exit the flow is considered thermally fully developed

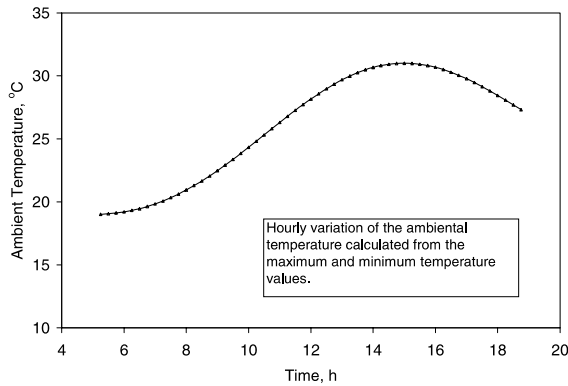


Fig. 3. Predicted hourly variation of the ambient temperature.

$$\frac{\partial T}{\partial x} = 0 \text{ in } x = x_3, \quad y_1 \leq y \leq y_2 \quad (24)$$

Considering the system initially in thermal equilibrium and stationary, the initial conditions are:

$$T = T_{\text{int}} \text{ in } t = 0 \quad (25)$$

$$u = v = 0 \text{ in } t = 0 \quad (26)$$

The ambient temperature is calculated based upon ASHRAE [33], where the hourly ambient temperature can be calculated from the maximum and minimum values by the equation

$$T_{\text{amb}}(t) = T_{\text{max}} - \frac{f}{100}(T_{\text{max}} - T_{\text{min}}) \quad (27)$$

where f is a factor obtained from ASHRAE [33] while the values of the maximum and minimum temperatures are obtained from the local meteorological data. Fig. 3 shows a curve of the hourly variation of the ambient temperature obtained by the above model, based upon the average monthly temperatures as well as the maximum and minimum values for the month of January in the city of Campinas.

3. Numerical solution

The present problem is solved numerically because the system of equations and the associated boundary conditions are complex without any available analytical solution.

Considering that the problem is two-dimensional the discretization of the governing equations by using an implicit scheme produces a system of coupled algebraic equations that must be solved simultaneously. When writing this system in a matrix form, one obtains a matrix with elements concentrated along five diagonal known as pent-diagonal. As an alternative method to avoid a pent-diagonal matrix, one can use the discretization scheme ADI (alternating direction implicit), where each time step is achieved in two time steps. In this man-

ner the ADI method treats implicitly one direction each time and produces two triadiagonal systems that can be solved efficiently by using TDMA (triadiagonal matrix algorithm).

Eqs. (8) and (10), written in finite difference by using implicit scheme and the ADI method, result in a system of equations adequate for the calculation of the velocity components u and v in the channel region, except at some singular points such as those situated at the channel exit or near the walls. These points need a special attention, since at and/or near them the boundary conditions for the momentum equations are specified and hence need to be treated separately. Similarly, the discretization of the energy equation, Eq. (11), using the ADI method and the resulting equations are valid for all points including neighbor points to entry and exit regions. It is worth remembering that the temperature at the entry point is equal to the temperature of the internal ambient and that the variation in temperature at exit is zero. The general computational grids are shown in Fig. 4.

To solve the system of discretized equations and their respective boundary conditions, an algorithm of solution based upon Fortran 90 is implemented. In this problem the velocity and temperature fields are coupled and consequently this fact must be taken into account when solving the system of equations. Also the pressure and velocity fields are coupled and this makes the solution more complex. The developed algorithm uses the method SIMPLE (Semi Implicit Linked Equations) to treat the pressure–velocity coupling. In this method, the velocities calculated during one intermediate step are corrected by the pressure field which must satisfy the mass conservations principle. As a result of using the SIMPLE method, an iteration process is realized in each time step and consequently needs a convergence criterion. The criterion used in this study to monitor the velocity and temperatures establishes that the maximum relative difference of the variables (u, v, T) in two successive iterations must be smaller than 1×10^{-4} , $\text{MAX}|(\phi^{\text{iter}+1} - \phi^{\text{iter}})/\phi^{\text{iter}+1}| \leq 1 \times 10^{-4}$, with $\phi = u, v, T$. Additionally the mass flux is monitored in each iteration, such that the maximum relative variation in two successive iterations is not more than 1×10^{-3} .

Points on the interface fluid external glass, points on the interface between the channel flow and the surface of the internal glass sheet, points at the corners and the adiabatic surfaces at entry and exit of the flow channel need a special treatment and is omitted here for the sake of brevity.

4. Validation of the model

In order to optimize the computational code and achieve convergence and stability independent of the grid size, numerical tests were realized considering the two glass sheets of 8 mm thickness and 1 m length each

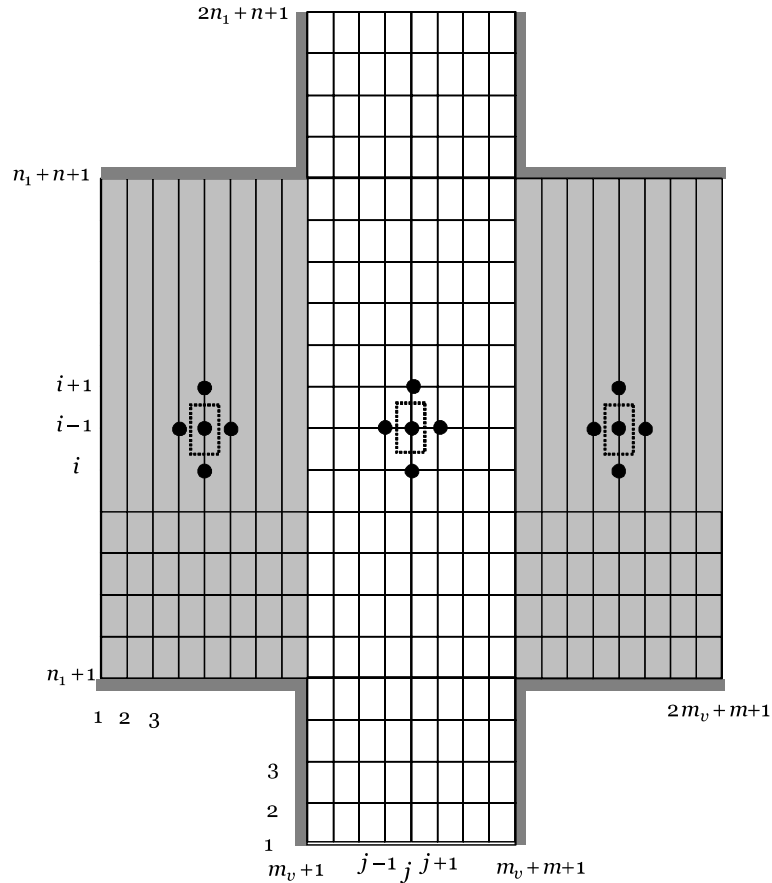


Fig. 4. Computational grids for the glass sheets and the fluid in the channel.

separated by a 3 cm gap, receiving constant solar radiation of 600 W/m^2 and subject to internal and external ambient temperatures of 24°C and 35°C respectively. The emissivity of the glass material is considered as 0.84. Axial grid intervals tested are 50, 76, 100 and 126, while keeping the transversal grid intervals constant. It was found that a number of axial intervals of 100 are sufficiently good. The number of axial intervals is fixed as 100 and also the number of intervals across the glass sheets is fixed at 10 grid intervals while varying the number of transversal grid intervals from 10 to 50. The results, omitted here for brevity, confirm that 50 grid intervals across the channel are good enough. The time step was also varied from 0.001 to 0.05. The results indicated that time step must be equal or smaller than 0.01 s. Hence 0.01 s was used in the numerical simulations. In summary, 100 intervals along the channel length and 50 intervals across, being 10 across the first glass, 30 across the channel and another 10 across the second glass. The time step used is 0.01 s.

Beside the computation grid tests and its optimization, it is a necessary to validate the computational code, before it is used to calculate the parameters of the pre-

sent problem. There are some possibilities of validating the numerical program. One possibility is to compare the numerical findings with experimental results realized specifically under the same geometrical and operational conditions. Also it is possible to compare the present numerical findings with available numerical and experimental results available in the literature. Another option is to simulate classical study cases for which analytical solutions or experimental results are available.

In the present study it was decided to simulate a similar problem investigated by other authors with well accepted available results. The chosen problem is of natural convection between parallel vertical plates under constant temperature and constant heat flux boundary conditions investigated by Aung et al. [34]. In their work, the authors realized a numerical experimental study of laminar flow between parallel plates caused by natural convection. They formulated the problem using a steady state model. Since the present model is transient, the simulations were extended until reaching the steady regime in order to be able to compare with their results. The parameter chosen for comparison is the induced dimensionless volumetric flow rate calcu-

lated for the cases of symmetrical heating under the two conditions of uniform temperature and uniform heat flux.

Figs. 5 and 6 show the numerical predictions from the present model compared with the results due to Aung et al. [34] for the case of constant wall temperatures and constant heat flux respectively. As can be seen the agreement is very good.

Wirtz and Stutzman [35] in their work presented experimental results for the natural convection induced flow between parallel vertical plates. The plates were heated symmetrically by a uniform and constant heat flux and the wall surface temperature was measured by thermocouples.

Fig. 7 shows the comparison between the predictions from the present model and their experimental results

for the cases of constant heat flux of 55.68 W/m^2 and 114.24 W/m^2 . The agreement seems to be good.

5. Calculations of the thermal performance parameters

The thermal efficiency of glass windows is usually presented in terms of the global heat transfer coefficient U and the overall thermal resistance of the window system (R). In both cases the values calculated or tested must be in agreement with the ASHRAE Standard [34] and must include the contribution of all elements of the window system. In calculating the value of U , the contribution from the glass frame, boundary and attachments must be included together with the external and internal convection heat transfer coefficients.

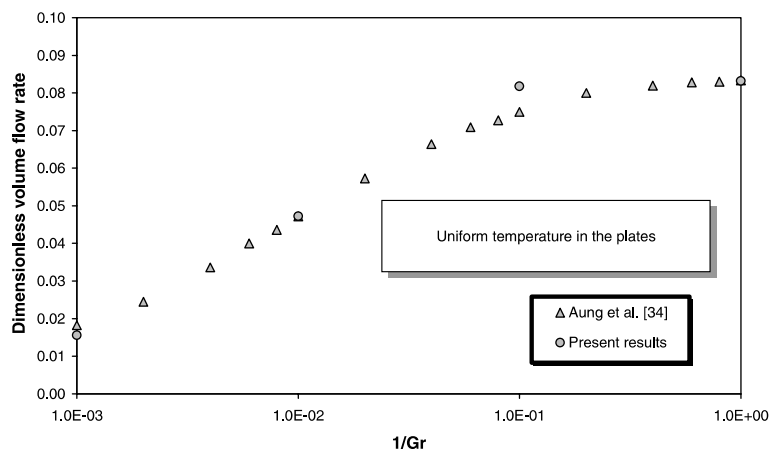


Fig. 5. Dimensionless flow rate for constant wall temperature.

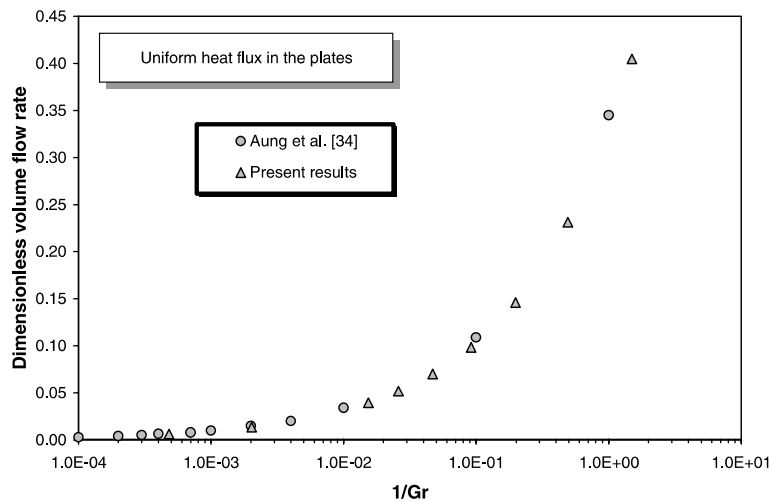


Fig. 6. Dimensionless flow rate for uniform heat flux at the walls.

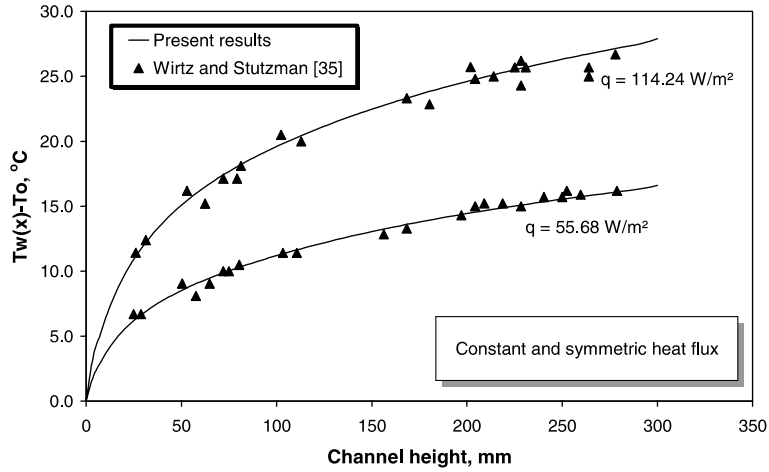


Fig. 7. Comparison between results of the present model with experimental results from Wirtz and Stutzman [35] for $q = 55.68 \text{ W/m}^2$ and $q = 114.24 \text{ W/m}^2$.

For the case of multiple glass sheets, the internal filling gases must be accounted for. In the case of multiple glass window system the overall heat transfer coefficient given by

$$U = \frac{1}{\frac{1}{h_{ext}} + \sum_{j=1}^N \frac{e_j}{k_j} + \sum_{j=1}^{N-1} \frac{1}{h_{c,j}} + \frac{1}{h_{int}}} \quad (28)$$

where N is the number of glass sheets and the $h_{c,j}$ is the cavity coefficient of heat transfer.

The coefficient of heat gain due to incident solar radiation is an important index for ranking glass window. This coefficient is defined as the fraction of incident solar radiation which enter the internal ambient as heat and is composed of two components. The first component is the solar radiation crossing the window and absorbed by the internal ambient while the second component is the solar radiation absorbed into the glass sheets and transferred to the internal ambient by heat transfer mechanisms. The first component is determined from calculations involving the optical properties of the system and solar radiation data. In residential glass window this component is dominant since these windows are usually designed to have high transmittance in the visible range and consequently will have good transmittance for solar radiation. The second component is determined by solar optical analysis as well as heat transfer analysis.

Part of the solar radiation absorbed by the glass window crosses directly to the internal ambient and its magnitude depends upon the total thermal resistance of the glass window. The total energy entering the internal ambient depends upon the geometrical parameters of the window, the thermal and optical properties of the window system materials. Hence the calculation of solar heat gain coefficient F must include the glass area A_v , frame area A_{fr} and other elements of the window and is given by

$$F = \frac{A_v F_v + A_{fr} F_{fr} + \sum A_j F_j}{A_g + A_{fr} + \sum A_j} \quad (29)$$

where j represent the other elements of the window system. In general the contribution of other elements to the value of F is of the order of 0.01 in case of wooden frames and 0.02–0.03 in the case of aluminum frames.

The equation for calculating F can be obtained from the energy balance on the window whose equivalent thermal circuit is shown in Fig. 8. By writing the equality

$$(T_{ext} - T_{int}) = (T_{ext} - T_{1,ext}) + (T_{1,ext} - T_{1,int}) + (T_{1,int} - T_{2,ext}) + (T_{2,ext} - T_{2,int}) + (T_{2,int} - T_{int}) \quad (30)$$

and using the corresponding equivalent thermal circuit one can write the final equation in terms of q_5 as

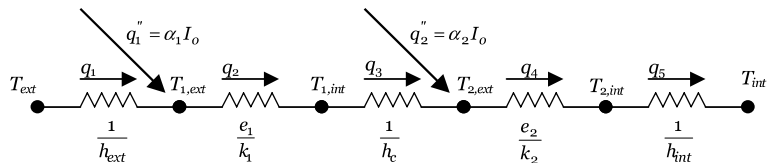


Fig. 8. Heat fluxes through a double glass window and the corresponding thermal circuit.

$$(T_{ext} - T_{int}) = q_5 \left(\frac{1}{h_{ext}} + \frac{e_1}{k_1} + \frac{1}{h_c} + \frac{e_2}{k_2} + \frac{1}{h_{int}} \right) - \frac{(\alpha_1 + \alpha_2)I_o}{h_{ext}} - \frac{\alpha_2 I_o e_1}{k_1} - \frac{\alpha_2 I_o}{h_c} \quad (31)$$

where α_1 and α_2 represent the absorptance coefficient of the external and internal glass respectively. The terms multiplied by q_5 in the Eq. (31) represent the inverse of the overall heat transfer coefficient U and the equation can be written as

$$q_5 = U(T_{ext} - T_{int}) + \frac{\alpha_1 I_o}{h_{ext}} U + \alpha_2 I_o \left[\frac{U}{h_{ext}} + \frac{Ue_1}{k_1} + \frac{U}{h_c} \right] \quad (32)$$

Equation (32) represent part of the heat admitted to the internal ambient. The first term on the right hand side of Eq. (32) represents the energy flux due to the temperature difference between the external and internal ambient, while the second and third terms represent the energy flux redirected to the internal ambient after part of the incident solar energy is absorbed by the two glass sheets. The expression of the total heat gain must also include the solar radiation transmitted directly to the internal ambient, that is $q = q_5 + \tau_{total}I_o$ or

$$q = U(T_{ext} - T_{int}) + \frac{\alpha_1 I_o}{h_{ext}} U + \alpha_2 I_o \left[\frac{U}{h_{ext}} + \frac{Ue_1}{k_1} + \frac{U}{h_c} \right] + \tau_{total}I_o \quad (33)$$

If one needs to calculate the energy admitted to the internal ambient due to incident radiation, the first term on the right side of Eq. (33) is omitted and the resulting equation becomes

$$q_{solar} = \frac{\alpha_1 I_o}{h_{ext}} U + \alpha_2 I_o \left[\frac{U}{h_{ext}} + \frac{Ue_1}{k_1} + \frac{U}{h_c} \right] + \tau_{total}I_o \quad (34)$$

To calculate the coefficient of solar heat gain (F), Eq. (34) is divided by the incident solar radiation I_o , to obtain

$$F = \frac{\alpha_1}{h_{ext}} U + \alpha_2 \left[\frac{U}{h_{ext}} + \frac{Ue_1}{k_1} + \frac{U}{h_c} \right] + \tau_{total} \quad (35)$$

Under transient conditions, the total heat gain can be calculated by energy balance in the form

$$q_{total} = \frac{1}{n\Delta x} \sum_{i=1}^n h_{int} \Delta x (T_{i,2m_c+m+1} - T_{int}) + \sigma_i \Delta x (T_{i,2m_c+m+1}^4 - T_{int}^4) + \tau_{total} I_o \Delta x \quad (36)$$

where the subscript i refers to a given element of the grid in the x -direction of the internal surface of the internal glass sheet. The sum of the energy balances over each element allows calculating the total heat gain (q_{total}). The solar heat gain can be obtained indirectly by calculating the heat gain with and without solar radiation and subtracting one from the other and dividing the result by the incident solar radiation as

$$q_{solar} = q_{total \text{ with } I_o} - q_{total \text{ without } I_o} \quad (37)$$

$$F = \frac{q_{total \text{ with } I_o} - q_{total \text{ without } I_o}}{I_o} \quad (38)$$

The shading coefficient (SC) is the second most important parameter for comparing and ranking glass window systems. The concept of the shading coefficient was developed to indicate how the coefficient of solar

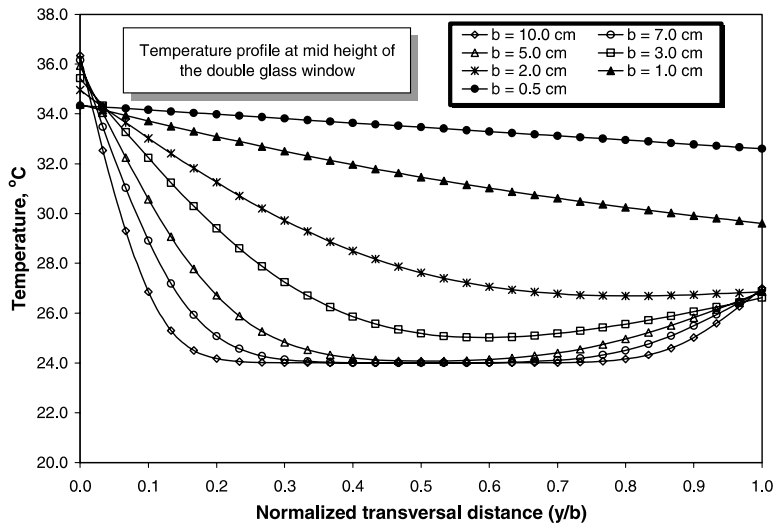


Fig. 9. Variations of the temperature profiles at window mid height with the normalized distance across the window.

gain of certain glass window system differs from the heat gain of a simple clear glass window system adopted as a reference system. In this manner SC can be written as

$$SC = \frac{F_{\text{glass window system}}}{F_{\text{reference}}} \quad (39)$$

Thus in order to calculate the shading coefficient SC it is necessary to define a reference system and determine its solar heat gain coefficient, $F_{\text{reference}}$. The reference system is defined according to ASHRAE Fundamentals [36] as a simple glass window system whose glass is of the type DSA (Double Strength Sheet Glass) of 3.175mm thickness and which has transmittance of a

0.86, reflectance of 0.08 and absorbance of 0.06 for normal incidence solar radiation. The internal and external heat convection coefficients are also defined resulting in a value of $U/h_{\text{ext}} = 0.17$ and $F_{\text{reference}} = 0.87$.

6. Discussion of results

Having realized the validation of the model, the numerical code was used to investigate the effects of the channel width on the velocity and the temperature fields, the total heat gain, coefficient of solar heat gain and the shading coefficient. In this analysis the glass

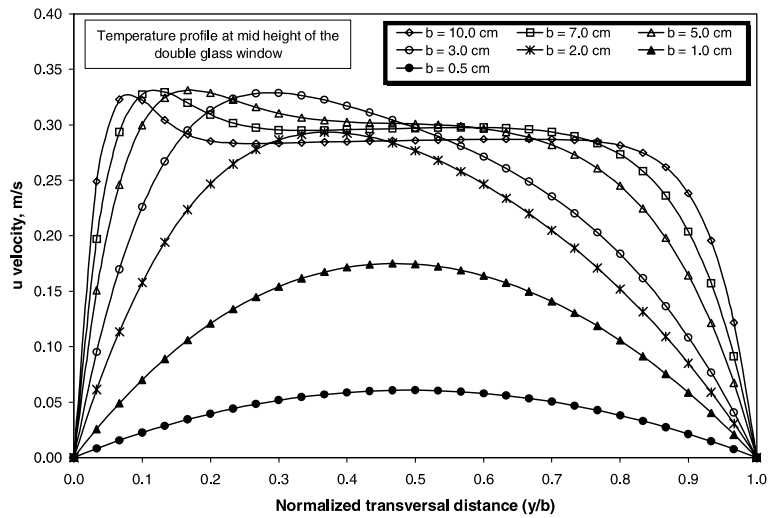


Fig. 10. Variation of the velocity profiles u at window mid height with the normalized distance across the window.

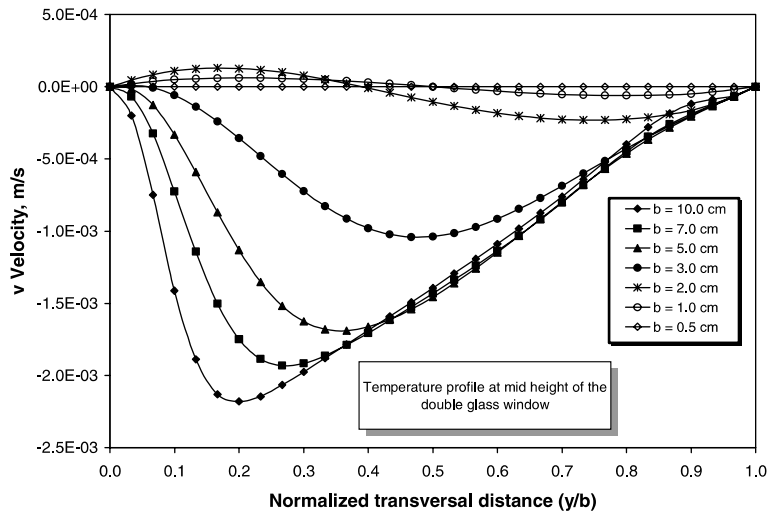


Fig. 11. Variation of the velocity profiles v at window mid height with the normalized distance across the window.

sheets considered are of 0.008m thickness and 1m length, with two equal adiabatic regions at entry and exit of 12.5% of the glass sheet length, internal and external ambient temperatures of 24°C and 35°C, emissivity of glass materials $\epsilon = 0.84$, extinction coefficient of 7.64m^{-1} under constant solar radiation of 600W/m^2 .

The results of the effect of the channel width on the temperature field at mid height of the channel under steady state conditions are shown in Fig. 9. As can be seen when the gap is small the temperature profile across the spacing seems to be linear indicating the situation of pure diffusion.

Fig. 10 shows the velocity profiles across the channel for different channel widths. As can be seen the velocity

increases as the gap width increases and changes from symmetric profile to non-symmetric when the gap is more than $b = 0.01\text{m}$. Similar comments can be made with respect to Fig. 11 for the velocity component v .

One important question is to analyze and verify whether the regime the induced flow in the channel under the conditions imposed in the present work is laminar or turbulent.

By the verification of the velocity fields one can conclude that for spacing between plates of 0.5cm the Reynolds number (based upon the spacing between the plates) is $Re_b = 12$, for $b = 3\text{cm}$ $Re_b = 416$, for $b = 7\text{cm}$ $Re_b = 1120$ and for $b = 10\text{cm}$ $Re_b = 1600$. Comparing these values of Re_b with the value of $Re_b = 1400$

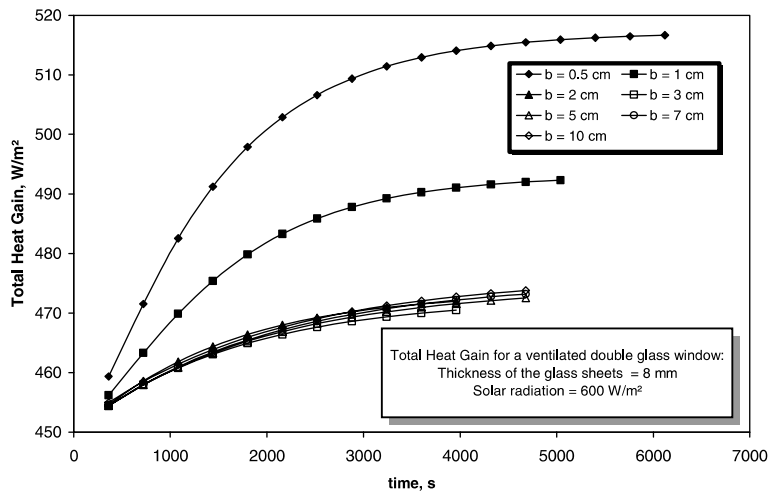


Fig. 12. Effect of the gap width on the total heat gain of a ventilated double glass window.

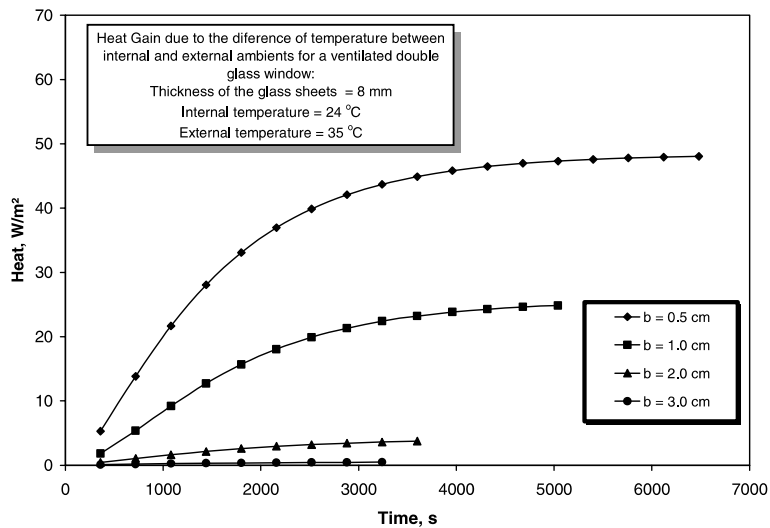


Fig. 13. Effect of the gap width on the heat gain due to temperature difference for a ventilated double glass window.

considered as the transition value of laminar to turbulent flow between parallel infinite plates, one can conclude that for all the spacings considered here the regime is laminar, except the case of 10cm where the validity is doubtful.

Fig. 12 shows the total heat gain for different values channel width. As can be seen, for channel width of 0.02m and higher values the total heat gain remains nearly unaltered.

Ignoring at least for the moment, the solar radiation, the heat gain or loss due to the temperature difference between the internal and the external temperatures depends upon the thermal resistance of the window components. Fig. 13 shows the heat gain due to the temperature difference in terms of the gap between the window sheets. As can be seen the increase of the size of the gap leads to increasing the thermal resistance.

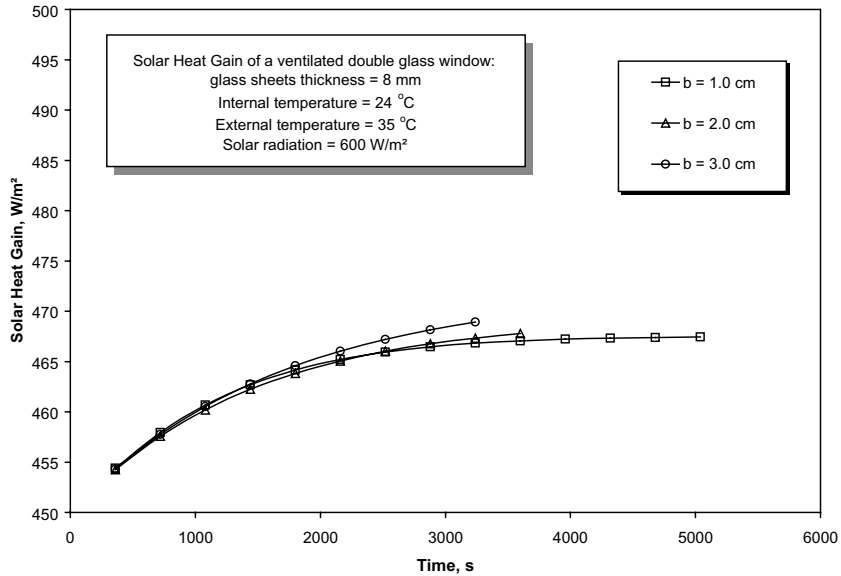


Fig. 14. Effect of the gap width on the solar heat gain of a ventilated double glass window.

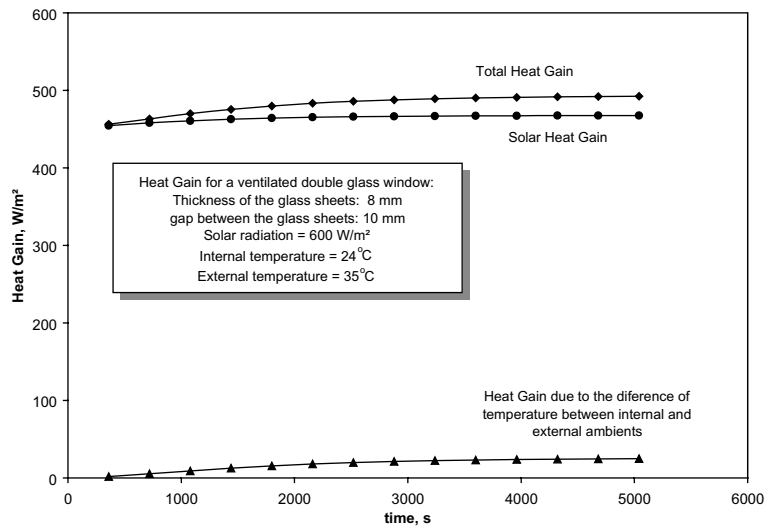


Fig. 15. Different heat gains for a ventilated double glass window of 5mm thick glass.

Frequently, it is interesting to know exclusively the heat gain due to the solar radiation. This heat gain is composed of two components; the heat gain due to incident solar radiation which crosses directly to the internal ambient. The second component of the heat gain is due to solar radiation absorbed by the glass sheets and reemitted to the internal ambient. Fig. 14 shows the solar heat gain for three different values of channel width. As can be seen there is a little difference between the solar heat gain of the three arrangements. This can be

attributed to the fact that the optical transmittance of the arrangements is nearly the same. Since the dominant component of the solar heat gain is influenced directly by the optical transmittance, as can be confirmed from Fig. 15, the three curves are nearly the same. The integration of the curves of the Solar Heat Gain with respect to time to obtain the mean values which when normalized by the incident solar radiation one can obtain the heat gain coefficient. When the coefficients of solar heat gain are normalized in relation to the solar heat gain of a

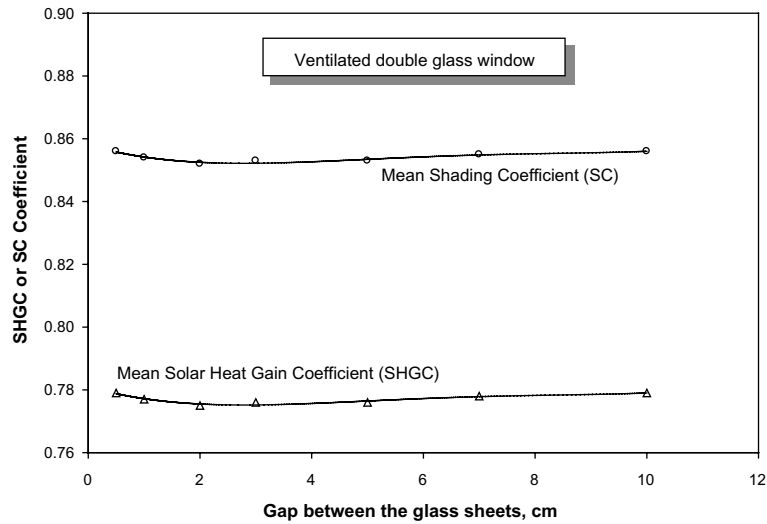


Fig. 16. Effect of gap width on the mean solar heat gain and shading coefficients for a ventilated double glass window.

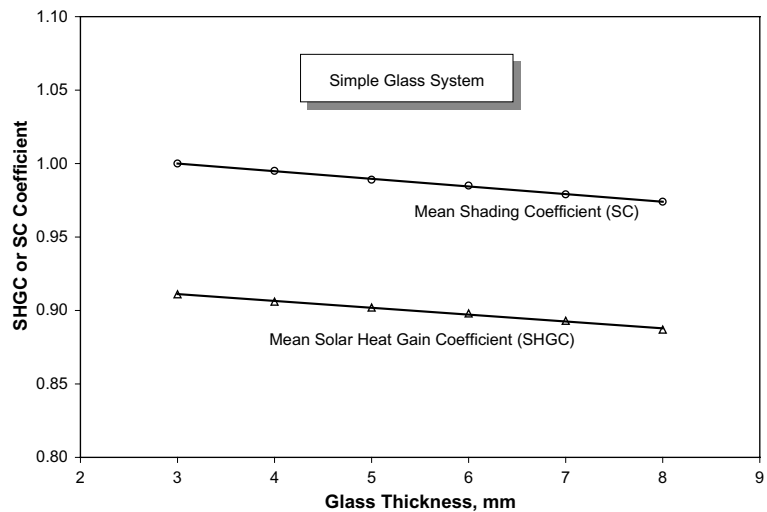


Fig. 17. Effect of gap width on the mean solar heat gain and shading coefficients for a simple glass system.

reference system, one can obtain the shading coefficients. The system adopted as a reference system is the simple glass window of a 0.003 m glass thickness.

Fig. 16 presents the results of the mean coefficient of solar heat gain and the shading coefficient for a ventilated double-sheeted glass window in terms of the gap between the glass sheets. One can observe that the curve is essentially constant of value 0.77, compared to the value of 0.88 obtained for the case of simple glass window of 0.008 m glass thickness. As can be seen the double glass window system is thermally more efficient than the single glass system having a constant value of the shading coefficient of 0.85 as can be verified from comparing Figs. 16 and 17.

7. Conclusions

A mathematical model is developed to simulate the thermal behavior of ventilated double glass window. The model takes into account the physical phenomena present in the heat and flow processes and also the real boundary conditions while in normal operation.

The numerical simulations were compared with available results and the agreement was found satisfactory. Effects of the gap width on the temperature distribution, the velocity field, the coefficient of the total heat gain, the coefficient of the solar heat gain and the shading coefficient were investigated.

The results indicate that the gap width has little effect on the mean coefficient of solar heat gain and the mean shading coefficient.

Acknowledgments

The authors wish to thank the Brazilian National Research Council for the scholarships and the financial support.

References

- [1] C.M. Lampert, Heat mirror coatings for energy conserving windows, *Solar Energy Mater. Solar Cell* 6 (1981) 1–41.
- [2] R.R. Dahlen, Low-e films for window energy control, *ASHRAE Trans.* 93 (part 1) (1987) 1517–1524.
- [3] P.J. Sebastian, V. Sivaramakrishnan, CdSe thin films as solar control coatings, *Solar Energy Mater. Solar Cell* 27 (1992) 321–326.
- [4] P.J. Sebastian, M. Pattabi, Solar control characteristics of Cu₂Se coating, *J. Phys. D: Appl. Phys.* 25 (1992) 981–985.
- [5] G. Alvarez, D.N. Jiménez, C.A. Estrada, C.A. Thermal performance of solar control coatings: a mathematical model and its experimental verification, *J. Phys. D: Appl. Phys.* 31 (1998) 2249–2257.
- [6] G. Alvarez, J.J. Flores, C.A. Estrada, The thermal response of laminated glass with solar control coating, *J. Phys. D: Appl. Phys.* 31 (1998) 3057–3065.
- [7] R. Sullivan, D.K. Arasteh, F.A. Beck, S.E. Selkowitz, Energy performance of evacuated glazing in residential buildings, *ASHRAE Trans.* 102 (part 2) (1996) 220–227.
- [8] M. Lenzen, R.E. Collins, Long-term field tests of vacuum glazing, *Solar Energy* 61 (1) (1997) 11–15.
- [9] R.E. Collins, T.M. Simko, Current status of the science and technology of vacuum glazing, *Solar Energy* 62 (3) (1998) 189–213.
- [10] S. Reilly, D. Arasteh, M. Rubin, The effects of infrared absorbing gasses on window heat transfer: a comparison of theory and experiments, *Solar Energy Mater.* 20 (1990) 277–288.
- [11] M.A. Bernier, B. Bourret, Effects of glass plate curvature on the U-factor of sealed insulated glazing units, *ASHRAE Trans.* 103 (part 1) (1997) 270–277.
- [12] Y. Zhao, W.P. Goss, D. Curcija, Prediction of the multicellular flow regime of natural convection in fenestration glazing cavities, *ASHRAE Trans.* 103 (part 1) (1997) 1009–1020.
- [13] M. Einarsrud, S. Haereid, V. Wittwe, Some thermal and optical properties of a new transparent silica xerogel material with low density, *Solar Energy Mater. Solar Cell* 31 (1993) 341–347.
- [14] K. Duer, S. Svendsen, Monolithic silica aerogel in super-insulating glazings, *Solar Energy* 63 (4) (1998) 259–267.
- [15] J.N.C. Castro, Paredes térmicas, Doctorate thesis, Universidade Estadual de Campinas, Campinas-SP, Brazil, 1991.
- [16] J.R. Henríquez, Estudo numérico e experimental sobre vidros térmicos, Master Thesis, Universidade Estadual de Campinas, Campinas-SP, Brazil, 1996.
- [17] K.A.R. Ismail, J.R. Henríquez, U-values, optical and thermal coefficients of composite glass systems, *Solar Energy Mater. Solar Cells* 52 (1998) 155–182.
- [18] K.A.R. Ismail, J.R. Henríquez, Thermally effective windows with moving phase change material curtains, *Appl. Thermal Eng.* 21 (2001) 1909–1923.
- [19] H. Manz, P.W. Egolf, P. Suter, A. Goetzberger, TIM-PCM external wall system for solar space heating and daylighting, *Solar Energy* 61 (6) (1997) 369–379.
- [20] K. Rottkay, M. Rubin, J. Kerr, Optical modeling of a complete electrochromic device, In: *Proc 2nd Int Conf Electrochromics*, San Diego, USA, 1996.
- [21] A. Seeboth, J. Schneider, A. Parzak, Material for intelligent sun protecting glazing, *Solar Energy Mater. Solar Cells* 60 (2000) 263–277.
- [22] N. Onur, M. Sivrioglu, O. Turgut, An experimental study on air window collector having a vertical blind for active solar heating, *Solar Energy* 57 (5) (1996) 375–380.
- [23] TEPSCO. Ventilation windows and automatic blinds help to control heat and lighting, *CADDET* (http://www.caddet-ee.org/newsdesk/nw498_03.htm) *Energy Efficiency Newsletter* (4) (1998) 9–11.
- [24] Y. Etzion, E. Erell, Controlling the transmission of radiant energy through windows: a novel ventilated reversible glazing system, *Building and Environ.* 35 (2000) 433–444.
- [25] J. Tanimoto, K. Kimura, Simulation study on an air flow window system with an integrated roll screen, *Energy and Buildings* 26 (1997) 317–325.

- [26] K.H. Haddad, A.H. Elmahdy, Comparison of the monthly thermal performance of a conventional window and a supply-air window, *ASHRAE Trans.* 104 (part 1B) (1998) 1261–1270.
- [27] Z. Zhang, A. Bejan, J.L. Lage, Natural convection in a vertical enclosure with internal permeable screen, *J. Heat Transfer* 113 (1991) 377–383.
- [28] S. Belharat, G. Desrayaud, G. Lauriat, Natural convection-radiation interaction in vented double glazing, in: *Proceeding of the 2nd European Thermal-Sciences and 14th UIT National Heat Transfer Conference*, Roma, Italy, 1996, pp. 811–818.
- [29] P.F. Abreu, A.F. Roydon, H.F. Sullivan, J.L. Wright, A 2-D numerical model for heat transfer calculations in multipane windows, in: *Proc VII Encontro Nacional de Ciências Térmicas-ENCIT*, Rio de Janeiro, Brazil, 1998, 59–64.
- [30] U. Larsson, B. Moshfegh, M. Sandberg, Thermal analysis of super insulated windows (numerical and experimental investigations), *Energy and Buildings* 29 (1999) 121–128.
- [31] J.R. Henríquez, *Modelagem e análise de janelas térmicas*, Doctoral thesis, Universidade Estadual de Campinas, Campinas-SP, Brazil, 2002.
- [32] F. Marcondes, C.R. Maliska, Convecção natural elíptica em canais de forma arbitrária. In: *XI Congresso Brasileiro de Engenharia Mecânica*, São Paulo, Brasil, 1991, pp. 5–8.
- [33] ASHRAE, *Handbook of Fundamentals*. American Society of Heating, Refrigerating and Air-Conditioning Engineers, Inc., USA, 1985.
- [34] W. Aung, L.S. Fletcher, V. Sernas, Developing laminar free convection between flat plates with asymmetric heating, *Int. J. Heat Mass Transfer* 15 (1972) 2293–2308.
- [35] R.A. Wirtz, R.J. Stutzman, Experiments on free convection between vertical plates with symmetric heating, *J. Heat Transfer* 104 (1982) 501–507.
- [36] ASHRAE, *Handbook of Fundamentals—Chapter 27: Fenestration*. American Society of Heating, Refrigerating and Air-Conditioning Engineers, Inc., USA, 1993.